BNL-73899-2005-IR

Neutron-proton effective range parameters and zero-energy shape dependence

Robert W. Hackenburg

June 2005

XXX Physics Department XXX

Brookhaven National Laboratory
P.O. Box 5000
Upton, NY 11973-5000
www.bnl.gov

Managed by
Brookhaven Science Associates, LLC
for the United States Department of Energy under
Contract No. DE-AC02-98CH10886

This is a preprint of a paper intended for publication in a journal or proceedings. Since changes may be made before publication, this preprint is made available with the understanding that it will not be cited or reproduced without the permission of the author.

DISCLAIMER

This report was prepared as an account of work sponsored by an agency of the United States Government. Neither the United States Government nor any agency thereof, nor any of their employees, nor any of their contractors, subcontractors, or their employees, makes any warranty, express or implied, or assumes any legal liability or responsibility for the accuracy, completeness, or any third party's use or the results of such use of any information, apparatus, product, or process disclosed, or represents that its use would not infringe privately owned rights. Reference herein to any specific commercial product, process, or service by trade name, trademark, manufacturer, or otherwise, does not necessarily constitute or imply its endorsement, recommendation, or favoring by the United States Government or any agency thereof or its contractors or subcontractors. The views and opinions of authors expressed herein do not necessarily state or reflect those of the United States Government or any agency thereof.

Printed on recycled paper

DRAFT BNL-73899-2005-IR

Neutron-proton effective range parameters and zero-energy shape dependence

R. W. Hackenburg*
Physics Department, Brookhaven National Laboratory, Upton, NY 11973
(Dated: June 14, 2005)

A completely model-independent effective range theory fit to available, unpolarized, np scattering data below 3 MeV determines the zero-energy free proton cross section $\sigma_0 = 20.4287 \pm 0.0078$ b, the singlet apparent effective range $r_s = 2.754 \pm 0.018_{\rm stat} \pm 0.056_{\rm syst}$ fm, and improves the error slightly on the parahydrogen coherent scattering length $a_c = -3.7406 \pm 0.0010$ fm. The triplet and singlet scattering lengths and the triplet mixed effective range are calculated to be $a_t = 5.4114 \pm 0.0015$ fm, $a_s = -23.7153 \pm 0.0043$ fm, and $\rho_t(0, -\epsilon_t) = 1.7468 \pm 0.0019$ fm. The model-independent analysis also determines the zero-energy effective ranges by treating them as separate fit parameters without the constraint from the deuteron binding energy ϵ_t. These are determined to be $\rho_t(0,0) = 1.705 \pm 0.023$ fm and $\rho_s(0,0) = 2.665 \pm 0.056$ fm. This determination of $\rho_t(0,0)$ and $\rho_s(0,0)$ is most sensitive to the sparse data between about 20 and 600 keV, where the correlation between the determined values of $\rho_t(0,0)$ and $\rho_s(0,0)$ is at a minimum. This correlation is responsible for the large systematic error in r_s. More precise data in this range are needed. The present data do not even determine (with confidence) that $\rho_t(0,0) \neq \rho_t(0, -\epsilon_t)$, referred to here as "zero-energy shape dependence". The widely used measurement of $\sigma_0 = 20.491 \pm 0.014$ b from W. Dilg, Phys. Rev. C **11**, 103 (1975), is argued to be in error.

PACS numbers: 13.75.Cs, 25.40.Dn, 29.85.+c

I. INTRODUCTION

The primary goals of this article are fourfold: first, using a model-independent analysis, to extract from the available data the best possible values of the effective range theory (ERT) parameters for np elastic scattering (the spin-triplet and spin-singlet scattering lengths a_t and a_s, and their effective ranges r_t and r_s, and the zero-energy free proton cross section σ_0 used to obtain those four); second, to obtain the best possible model-independent estimate of the mixed and zero-energy effective range difference $\rho_t(0,0) - \rho_t(0, -\epsilon_t)$; third, to demonstrate that there is a range of energy most sensitive to this difference (which turns out to be from about 20 keV to about 600 keV); and fourth, to demonstrate that better cross section measurements in this range are needed for a useful determination of this difference. The ERT parameters (especially σ_0), and this difference, have considerable relevance to nucleon-nucleon (NN) potential models.

Much of the work done in studying the NN interaction is done using models of the NN potential [1–4]. NN potential models have diverse low energy applications, such as studies of nuclear structure [5], neutrino detection [6], and pp weak capture [7], to name a few. NN potential models can also determine the ERT parameters. Partial wave analyses are used to fit the parameters of potential models to a large body of data including high energy data which do not bear directly on the low energy parameters. Thus, small, unnecessary errors may be introduced into the low-energy parameters obtained from these models. This is exacerbated when low energy data are omitted from the data sets [2]. If the data set is restricted to sufficiently low energies, where only the S wave is significant, an ERT analysis yields more accurate values for these parameters because it does not depend on mechanisms, nor on the shape of the nuclear potential, and is truly model-independent. Studies of charge independence [3, 8, 9], for example, use the np singlet parameters determined from an ERT analysis.

Some NN potential models use the free proton zero-energy cross section σ_0 as an input. Many of these use the 1975 measurement by Dilg [10], $\sigma_0 = 20.491(14)$ b. This value is deviant from all previous values, such as Houk's 1971 measurement $\sigma_0 = 20.436(23)$ b [11], but only by about two standard deviations or less, because of the larger uncertainties on the previous measurements. In 1990, Koester et al [12] determined $\sigma_0 = 20.420(10)$ b, which is in good agreement with Houk's result. With that small uncertainty, Dilg's value could no longer be accepted as being within two standard deviations of all other values. This should have laid the issue to rest, but the Koester et al value never seems to be used. To this day, some works simply use the Dilg measurement (e.g., [4, 8, 9]), either directly cited or indirectly (e.g., through [13, 14]), while some include both the Dilg and Houk measurements (e.g., [1–3, 7, 15, 16]). Meanwhile, unnecessarily inaccurate and inconsistent values for σ_0, and the resulting sets of ERT parameters, continue to be used. This is especially relevant to the low energy applications of NN potential models. The Appendix attempts to explain the problem with Dilg's result.

The remainder of this work deals with the simple, model-independent world of low energy data (S wave only), and an ERT analysis. This work analyzes a considerably larger body of data than previously used for this purpose, and the fit uncertainties are substantially

*hack@bnl.gov

reduced from previous determinations. Some improvements have been made to the method, including the handling of a correlation between the triplet and singlet effective ranges, which does not seem to have been previously treated. This correlation results in a substantial systematic error on the singlet effective range. By taking $\rho_t(0,0)$ and $\rho_s(0,0)$ as fit variables, without taking $\rho_t(0,0) = \rho_t(0,-\epsilon_t)$ and constraining it with the deuteron binding energy ϵ_t, it is possible to determine the triplet zero-energy effective range $\rho_t(0,0)$ separately from $\rho_t(0,-\epsilon_t)$ and without reference to a model. To obtain meaningful, statistical errors for $\rho_t(0,0)$ and $\rho_s(0,0)$ as fit variables, their correlation must be properly handled. Such a determination of $\rho_t(0,0)$ can tell us something about shape dependence (i.e., the shape of the nuclear potential), without any model-dependent assumptions.

II. EFFECTIVE RANGE THEORY SYNOPSIS AND ZERO-ENERGY SHAPE DEPENDENCE

The unpolarized, elastic np cross section σ is the spin-weighted sum of the noninterfering triplet and singlet partial cross sections, thus

$$\sigma = \tfrac{3}{4}\sigma_t + \tfrac{1}{4}\sigma_s. \tag{2.1}$$

ERT gives both the triplet and singlet S wave partial cross sections as [17–20]

$$\sigma_d = 4\pi/[(a_d^{-1} - \tfrac{1}{2}\rho_{dk}k^2)^2 + k^2], \tag{2.2}$$

where σ_d, a_d, ρ_{dk} are σ_t, a_t, ρ_{tk} for the triplet and σ_s, a_s, ρ_{sk} for the singlet, and where a_d is the scattering length and ρ_{dk} is the effective range. The center-of-mass (c.m.) momentum is k, with $k^2 = 2mT$ (nonrelativistically), where m is the reduced neutron-proton mass and where T is the c.m. np kinetic energy (in natural units: $\hbar = c = 1$). The relativistic relations actually used are given in (3.13) and (3.14).

Equation (2.2) is exact because it *defines* ρ_{dk}, which is shorthand for $\rho_d(0,T)$. In terms of the asymptotic (free particle) np wavefunction $v_d(T)$ and the exact (interacting) np wavefunction $u_d(T)$, both of which implicitly depend on the neutron-proton separation r, the function $\rho_d(T_a,T_b)$ is defined as [17–19]

$$\rho_d(T_a,T_b) \equiv 2\int_0^\infty dr\,[v_d(T_a)v_d(T_b) - u_d(T_a)u_d(T_b)]\,, \tag{2.3}$$

where ρ_d, v_d, u_d are ρ_t, v_t, u_t for the triplet and ρ_s, v_s, u_s for the singlet, and where T_a and T_b are any two values of the c.m. kinetic energy. This definition satisfies (2.2) exactly for $T_a = 0$ and $T_b = T$. The wavefunction u_d, but not v_d, depends on the shape of the nuclear potential, and this shape dependence manifests itself as energy dependence of ρ_d. All of this concerns only the S wave, so there is no angular dependence; the word *shape* refers to the dependence on r. The uncertainty principle prohibits us from probing the fine details of the potential at low energies. Therefore, the detailed shape of the nuclear potential can only have a small effect on the spectrum, as long as k^{-1} is much larger than the well size. Empirically, we know that the energy dependence of ρ_{dk} is small, at least for low energies. The *shape-independent approximation* replaces ρ_{dk} with the shape-independent effective range r_d (a constant), thus

$$\sigma_d \cong 4\pi/[(a_d^{-1} - \tfrac{1}{2}r_dk^2)^2 + k^2]. \tag{2.4}$$

For $T = -\epsilon_d$, where ϵ_d is the deuteron binding energy (ϵ_t for the triplet and ϵ_s for the singlet), we have the *mixed effective range* [21],

$$\rho_{dm} \equiv \rho_d(0,-\epsilon_d), \tag{2.5}$$

for which, exactly,

$$a_d^{-1} = \alpha_d - \tfrac{1}{2}\rho_{dm}\alpha_d^2 \quad \text{with} \quad \alpha_d \equiv \pm\sqrt{2m\epsilon_d}, \tag{2.6}$$

where the positive root is taken for the triplet, and the negative root for the singlet. The nonrelativistic form for α_d is shown, but the relativistic form (3.13) is used in the calculations, with $k^2 = -\alpha_d^2$ and $\epsilon_d = -T$. In the shape-independent ERT, for the triplet only, ρ_{tk} is taken as the constant $r_t = \rho_{tm}$, which satisfies (2.6) and is determined by a_t, ϵ_t, and the relation

$$\rho_{dm} = 2\alpha_d^{-1}\left(1 - 1/a_d\alpha_d\right), \tag{2.7}$$

which follows from (2.6). Since there is no measurement of ϵ_s, (2.7) cannot be used to obtain ρ_{sm}. Instead, r_s may be obtained from the three parameters a_t, a_s, r_t, and a measured elastic cross section σ_k at c.m. momentum k, through (2.1) and (2.4).

Consider that the *zero-energy effective range* $\rho_{d0} \equiv \rho_d(0,0)$ is a better approximation to $\rho_{dk} \equiv \rho_d(0,T)$ than is $\rho_{dm} \equiv \rho_d(0,-\epsilon_d)$, if shape dependence is admitted. At the very least, we have $\lim_{T\to 0}\rho_{dk} = \rho_{d0}$. While ρ_{t0} and ρ_{s0} may be calculated with specific assumptions of the triplet and singlet wavefunctions or potentials, it is both possible and important to extract estimates of these from data, without reference to a model. The relation between ρ_{d0} and ρ_{dm} is independent of the energy T. Define the constant Δr_d such that

$$\rho_{d0} \equiv \rho_{dm} + \Delta r_d. \tag{2.8}$$

The condition $\Delta r_t \neq 0$ is referred to in this article as "zero-energy shape dependence". Although a survey of nuclear-potential models exceeds the scope of this work, these models universally predict a nonzero value for Δr_t. Given sufficiently precise measurements, Δr_t can be used to discriminate between (or improve) these models. As will be seen, currently available measurements are not quite up to this task.

It is of some interest to obtain ϵ_s (specifying the pole position), which is done by solving (2.6) for ϵ_d, thus [22]

$$\alpha_d = \rho_{dm}^{-1}\left(1 \pm \sqrt{1 - 2\rho_{dm}/a_d}\right), \tag{2.9}$$

with ϵ_d following from (3.14), taking $k^2 = -\alpha_d^2$ and $\epsilon_d = -T$. Of course, ρ_{sm} is not known, so r_s must be employed.

III. ERROR ANALYSIS

The measurements and their uncertainties are:

$\sigma_0 \pm\delta\sigma_0$ the zero-energy elastic cross section
$a_c \pm\delta a_c$ the parahydrogen coherent scattering length
$\sigma_k \pm\delta\sigma_k$ the elastic cross section at c.m. momentum k.

The uncertainties $\delta\sigma_0$, δa_c, and $\delta\sigma_k$ are small and independent. Because its uncertainty is utterly negligible compared to the others, ϵ_t is taken as exact.

The zero-energy (free proton) elastic cross section is given by (2.1), taking $k = 0$ in (2.2), thus

$$\sigma_0 = \pi\left(3a_t^2 + a_s^2\right). \tag{3.1}$$

The parahydrogen coherent scattering length is [23]

$$a_c \equiv \tfrac{3}{2}a_t + \tfrac{1}{2}a_s. \tag{3.2}$$

The first group of derived quantities and their uncertainties are:

a_s $\pm\delta a_s$ the singlet scattering length
a_t $\pm\delta a_t$ the triplet scattering length
$\rho_{tm} \pm\delta\rho_{tm}$ the triplet mixed effective range.

These do not depend on σ_k. Only ρ_{tm} depends on ϵ_t. The formulas determining these, r_t, and r_s are

$$s \equiv \sqrt{\tfrac{1}{12}(\sigma_0/\pi - a_c^2)} \tag{3.3}$$

$$a_s = \tfrac{1}{2}a_c - 3s \qquad a_t = \tfrac{1}{2}a_c + s \tag{3.4}$$

$$r_t = \rho_{tm} + \Delta r_t \quad \rho_{tm} = 2\alpha_t^{-1}(1 - 1/a_t\alpha_t) \tag{3.5}$$

$$\sigma_t(k) \equiv 4\pi/[(a_t^{-1} - \tfrac{1}{2}r_t k^2)^2 + k^2] \tag{3.6}$$

$$\sigma_{sk} \equiv 4\sigma_k - 3\sigma_t(k) \tag{3.7}$$

$$r_s = 2k^{-2}(a_s^{-1} + \sqrt{4\pi/\sigma_{sk} - k^2}). \tag{3.8}$$

Equations (3.3) and (3.4) are exact, and follow from (3.1) and (3.2). The function $\sigma_t(k)$ is the theoretical triplet partial cross section; it is a shape-independent approximation if r_t is taken from (3.5). The quantity σ_{sk} is the estimated singlet partial cross section. Equations (3.7) and (3.8) follow from (2.1) and (2.4), and r_s is the singlet *apparent effective range*.

The determination of r_s from (3.8) contains contributions to its error from a_t, a_s, ϵ_t, σ_k, and, if using ρ_{tm} (instead of ρ_{t0}) as r_t, a systematic error from taking $\Delta r_t = 0$, and further systematic errors from ignoring the energy dependence of ρ_{tk} and ρ_{sk}. The latter may be eliminated, in principle to within any specified precision, by taking σ_k at a sufficiently low energy. The statistical uncertainty in r_s is

$$\delta r_s^2 = \left(\frac{\partial r_s}{\partial\sigma_0}\right)^2 \delta\sigma_0^2 + \left(\frac{\partial r_s}{\partial a_c}\right)^2 \delta a_c^2 + \left(\frac{\partial r_s}{\partial\sigma_k}\right)^2 \delta\sigma_k^2. \tag{3.9}$$

At this point, Δr_t is an unknown constant, and is presumed to be small. If Δr_t is ignored, using ρ_{tm} for r_t, then the singlet apparent effective range obtained will be the shape-independent value $r_s = r_{s0}$, with

$$r_{s0} \equiv \rho_{s0} - (\delta r_s)_{\Delta r_t} = \lim_{T\to 0} \rho_{sk} - (\delta r_s)_{\Delta r_t} \tag{3.10}$$

$$(\delta r_s)_{\Delta r_t} \equiv \int_{\rho_{tm}}^{\rho_{tm}+\Delta r_t} dr_t \left(\frac{\partial r_s}{\partial \Delta r_t}\right) = \left\langle \frac{\partial r_s}{\partial \Delta r_t}\right\rangle \Delta r_t.$$

TABLE I: The partial derivatives from (3.3) to (3.8).

$\frac{\partial a_s}{\partial\sigma_0} = \frac{-1}{8\pi s}$	$\frac{\partial a_t}{\partial\sigma_0} = \frac{1}{24\pi s}$	$\frac{\partial r_t}{\partial\sigma_0} = \frac{1}{12\pi s\alpha_t^2 a_t^2}$
$\frac{\partial a_s}{\partial a_c} = \frac{a_c}{4s} + \frac{1}{2}$	$\frac{\partial a_t}{\partial a_c} = \frac{-a_c}{12s} + \frac{1}{2}$	$\frac{\partial r_t}{\partial a_c} = \frac{2}{\alpha_t^2 a_t^2}\left(\frac{-a_c}{12s} + \frac{1}{2}\right)$
$\frac{\partial\sigma_t}{\partial\sigma_0} = \frac{-\sigma_t^2}{2\pi}\left(a_t^{-1} - \frac{1}{2}r_t k^2\right)\left[a_t^{-2}\left(\frac{\partial a_t}{\partial\sigma_0}\right) - \frac{1}{2}k^2\left(\frac{\partial r_t}{\partial\sigma_0}\right)\right]$		
$\frac{\partial\sigma_t}{\partial a_c} = \frac{-\sigma_t^2}{2\pi}\left(a_t^{-1} - \frac{1}{2}r_t k^2\right)\left[a_t^{-2}\left(\frac{\partial a_t}{\partial a_c}\right) - \frac{1}{2}k^2\left(\frac{\partial r_t}{\partial a_c}\right)\right]$		
$\frac{\partial\sigma_t}{\partial\Delta r_t} = \frac{\sigma_t^2 k^2}{4\pi}\left(a_t^{-1} - \frac{1}{2}r_t k^2\right)$		
$\frac{\partial r_s}{\partial\sigma_0} = \frac{-2}{a_s^2 k^2}\left(\frac{\partial a_s}{\partial\sigma_0}\right) + \frac{12\pi}{\sigma_{sk}^2 k^2\sqrt{(4\pi/\sigma_{sk}) - k^2}}\left(\frac{\partial\sigma_t}{\partial\sigma_0}\right)$		
$\frac{\partial r_s}{\partial a_c} = \frac{-2}{a_s^2 k^2}\left(\frac{\partial a_s}{\partial a_c}\right) + \frac{12\pi}{\sigma_{sk}^2 k^2\sqrt{(4\pi/\sigma_{sk}) - k^2}}\left(\frac{\partial\sigma_t}{\partial a_c}\right)$		
$\frac{\partial r_s}{\partial\sigma_k} = -16\pi/\sigma_{sk}^2 k^2\sqrt{(4\pi/\sigma_{sk}) - k^2}$		
$\frac{\partial r_s}{\partial\Delta r_t} = (3\sigma_t^2/\sigma_{sk}^2)(a_t^{-1} - \frac{1}{2}r_t k^2)/\sqrt{(4\pi/\sigma_{sk}) - k^2}$		

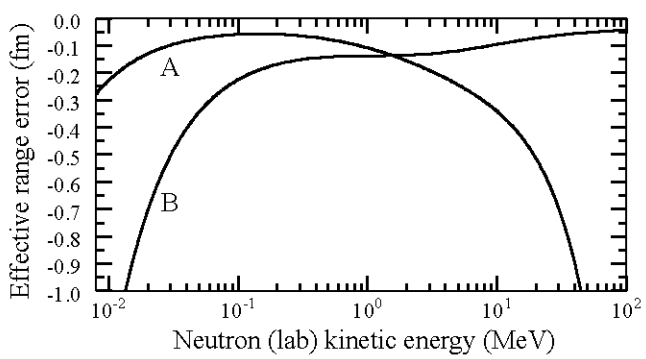

FIG. 1: Contribution to the error δr_s in the singlet apparent effective range r_s from the measurement error $\delta\sigma_k$ in the cross section σ_k, through $(\partial r_s/\partial\sigma_k)\delta\sigma_k$.
Curve A: $\delta\sigma_k = 0.01$ b, i.e., for fixed errors.
Curve B: $\delta\sigma_k = 0.003 \times \sigma_k$, i.e., for variable errors, 0.3% of cross section.

Table I shows the partial derivatives of the parameters a_t, a_s, r_t, r_s with respect to $\sigma_0, a_c, \sigma_k, \Delta r_t$. Figures 1 and 2 plot the contributions to δr_s from the errors $\delta\sigma_k$, $\delta\sigma_0$, and δa_c. In these figures, the curves are calculated using the theoretical partial cross section $\sigma_s(k)$ from (2.4).

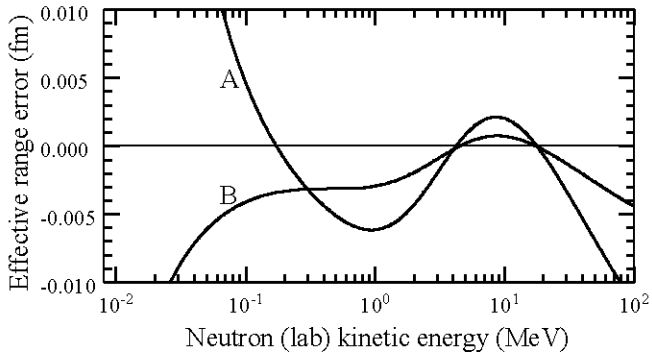

FIG. 2: Contributions to the error δr_s in the singlet apparent effective range r_s from the measurement errors $\delta\sigma_0$ and δa_c in σ_0 and a_c.
Curve A: contribution from $(\partial r_s/\partial\sigma_0)\delta\sigma_0$, for $\delta\sigma_0 = 0.01$ b.
Curve B: contribution from $(\partial r_s/\partial a_c)\delta a_c$, for $\delta a_c = 0.001$ fm.

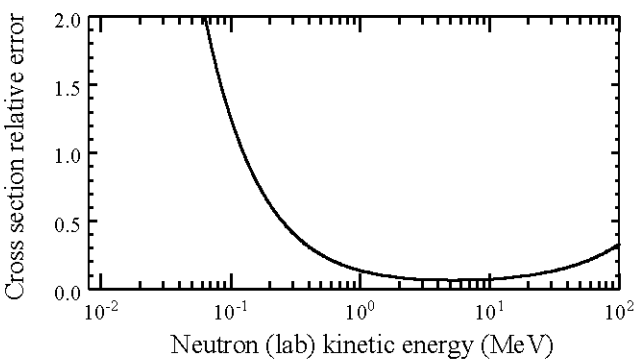

FIG. 3: Relative (or fractional) critical error size in the cross section, defined as $\delta\sigma_{\rm crit}/\sigma$ from (2.1), (2.4), (3.11). Measured cross sections which exceed the theoretical cross section by more than this produce nonsense (complex) values for r_s.

There is a *critical error size* $\delta\sigma_{\rm crit}$, which follows from (3.8), when the expression in the radical goes to zero, i.e., $4\pi/\sigma_{sk} = k^2$. This occurs for $\sigma_{sk} = \sigma_s(k) + 4\delta\sigma_{\rm crit}$, thus

$$\delta\sigma_{\rm crit} = \tfrac{1}{4}[4\pi/k^2 - \sigma_s(k)]. \tag{3.11}$$

This is plotted in Fig. 3 as a fractional error. Cross section measurements that exceed the theoretical value by more than this produce nonsense (complex) values for r_s from (3.8).

The form (2.4) yields $\lim_{T\to\infty}\sigma_d = 16\pi/r_d^2k^4$, so the expression in the radical of (3.8) should remain positive as $T\to\infty$. However, higher waves increase the cross section relative to (2.4), and it turns out that above about 100 MeV, the apparent effective range r_s cannot be calculated without subtracting higher waves.

Figure 4 plots the slope $\partial r_s/\partial\Delta r_t$, which describes how Δr_t affects r_{s0}.

The variables k, T, and T_L, where T_L is the neutron kinetic energy in the frame of the proton (lab), are used interchangeably as the independent variable in evaluating

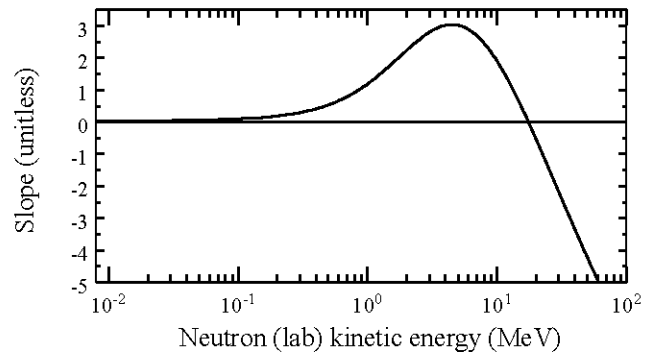

FIG. 4: Dependence of r_{s0} on Δr_t, plotted as $\partial r_s/\partial\Delta r_t$, from Table I. Note: $\lim_{T\to 0}\partial r_s/\partial\Delta r_t = -3a_t^3/a_s^3 = 0.03564$.

σ, σ_d, ρ_d, etc. The mappings $k \leftrightarrow T \leftrightarrow T_L$ employed in the calculations in this work are always the relativistic ones, thus, with $E \equiv m_n + m_p + T$,

$$k^2 = \frac{m_p^2 T_L(2m_n + T_L)}{(m_n+m_p)^2 + 2T_L m_p} \tag{3.12}$$

$$k^2 = \tfrac{1}{4}[E^2 - 2(m_n^2+m_p^2) + (m_n^2 - m_p^2)^2/E^2] \tag{3.13}$$

$$T = \sqrt{k^2 + {m_n}^2} - m_n + \sqrt{k^2 + {m_p}^2} - m_p \tag{3.14}$$

$$T_L = T(T + 2m_n + 2m_p)/2m_p. \tag{3.15}$$

Failure to use the relativistic relations for the deuteron binding energy results in about a 0.75 standard deviation shift down in the triplet mixed effective range.

The masses and other physical constants used here are from the 2004 PDG listing [24]: m_p = 938.272 029(80) MeV/c^2, m_n = 939.565 36(08) MeV/c^2, and $\hbar c$ = 197.326 968(17) MeV fm. The value used for ϵ_t is that from [25], ϵ_t = 2.224 566 14(41) MeV.

IV. THE FIT

Historically, the most used method for obtaining the ERT parameters starts with a direct determination of a_t, a_s, and r_t (as ρ_{tm}) from the three measured values $\sigma_0, a_c, \epsilon_t$, and the equations (3.3) to (3.5), leaving r_s undetermined. Any single measurement of a cross section at a nonzero energy determines r_s (as r_{s0}) from the equations (3.6) to (3.8), taking $\Delta r_t = 0$. Or, r_{s0} can be determined from a collection of such data using an LMS fit, which is equivalent to a weighted average of single-point determinations. In any case, σ_0 and a_c have all the influence on the parameters a_t, a_s, and ρ_{tm}, while the higher energy measurements have none.

The method for obtaining the shape-independent ERT parameters with a fit takes $\Delta r_t = 0$ and $r_t = \rho_{tm}$, constrained by a_t and ϵ_t with (3.5), and then fits the three remaining parameters, a_t, a_s, and r_s (as r_{s0}), to measurements of σ_0, a_c, and some set $\{\sigma_k\}$ of measured cross sections at higher energies [26]. This determination of a_t, a_s,

and r_{s0} differs only slightly, and not significantly, from their direct determination, mentioned above. It is, however, more flexible in that it can determine a_t, a_s, r_t, and r_s when the measurements of σ_0, a_c, and ϵ_t are singly or jointly omitted. In particular, fitting without employing ϵ_t permits $\rho_t(0,0)$ (and therefore Δr_t) to be determined, and this is not otherwise possible.

The fitting algorithm is described in [27]. Cross section measurements, including σ_0, contribute terms $w \times [\sigma(\text{fit}) - \sigma(\text{meas})]^2$ to χ^2, where w is the weight, with $w = 1/\delta^2$ from the measurement uncertainty δ, defined as a standard deviation of a Gaussian distribution. Measurements of a_c contribute terms $w \times [a_c(\text{fit}) - a_c(\text{meas})]^2$ to χ^2. The number of degrees of freedom ν is the number of data less the number of fit variables, and $\chi^2_\nu \equiv \chi^2/\nu$. For independent variables and Gaussian error distributions, the fit uncertainties are standard deviations, if $\chi^2_\nu = 1 \pm \sqrt{2/\nu}$ [28].

The correlation between the two fit parameters a_t and a_s presents a small difficulty. Two variables x and y are substantially correlated if the increase in χ^2_ν from a variation δx in x can be substantially cancelled by some opposing variation δy in y, where δx and δy are comparable in size to the standard deviations in x and y, or larger. When this situation exists, the fit errors from the fitter will *underestimate* the uncertainties in x and y. How much the uncertainties are underestimated depends on how large these opposing variations can be made compared to their respective standard deviations without χ^2_ν suffering a substantial increase from its minimum. Whether variables are substantially correlated with each other depends on the type, range of energy, and precision of the data to which they are fit. To avoid this difficulty, σ_0, a_c, and r_{s0} are taken as the fit variables, with a_t and a_s following from (3.4). Measurements of a_c so tightly constrain the fit value of a_c that it is practically fixed to that of a weighted average of the a_c measurements. The cross section measurements determine σ_0 and r_{s0}, with the lower energy measurements mainly affecting σ_0 and the higher energy measurements mainly affecting r_{s0}. The effect is that these fit parameters are for all practical purposes uncorrelated with each other.

A. Data selection

The measurements of σ_0 and a_c that were considered are shown in Tables II and III. The parameters used for calculating the χ^2 values shown are the shape-independent values from Sec. IV C, but the parameters from [12], $a_t = 5.411(3)$ fm, $a_s = -23.711(6)$ fm, $r_t = 1.745(5)$ fm, and $r_s = 2.76(5)$ fm from [29], yield similar χ^2 values. One measurement of σ_0 and two of a_c were excluded because they are substantially deviant from most of the other measurements, as evidenced by their large χ^2 values. The value of σ_0 from [12] is derived (mainly) from a pair of measurements at 1.97 keV and 143 keV. Since these two points are included in the cross section data used for the fits, it would not be correct to also include this value of σ_0.

TABLE II: The σ_0 data considered for the fits. Values with large χ^2 are excluded.

	Reference	Year	σ_0 (b)	χ^2	Included in fits?
[30]	Melkonian	1949	20.360(50)	1.89	Yes[a]
[11]	Houk	1971	20.436(23)	0.102	Yes
[10]	Dilg	1975	20.491(14)	19.8	No[b]
[12]	Koester	1990	20.420(10)	0.75	No[c]

[a]Error shown as adjusted by Engelke et al [31], 1963.
[b]See the Appendix.
[c]This value is derived mainly from a pair of cross section measurements which are included in the set of cross section data, so it would not be correct to include this value of σ_0.

TABLE III: The a_c data considered for the fits. Values with large χ^2 are excluded.

	Reference	Year	a_c (fm)	χ^2	Included in fits?
[11]	Houk	1971	−3.7210(40)	24	No
[32]	Koester	1971	−3.7400(30)	0.04	Yes
[33]	Callerame	1975	−3.7330(40)	14.4	No
[34]	Sears	1985	−3.7406(11)	0	Yes[a]

[a]Adjusted from Koester and Nistler [14], 1975.

Total cross section data were obtained from the Computerized Index to Neutron Data (CINDA) through Brookhaven National Laboratory's National Nuclear Data Center (NNDC) [35] and from the literature. These data are shown in Table IV. The parameters used for calculating the average χ^2 per datum shown in Table IV are the shape-independent values from Sec. IV C; the parameters from [12] yield similar χ^2. Data were not included that had no stated uncertainties or large uncertainties (more than 10% fractional error), or were from an unpublished thesis, or where the results were not expressed as np cross sections. The neutron capture cross sections σ_{M1} and σ_{E1} are assumed to be negligible and were not subtracted from the total cross sections. Higher waves were not subtracted. Corrections such as those for inscattering, system deadtime, detector efficiency, the presence of other nuclei, etc. are assumed to have already been made to the published data [66]. None of the data above 50 MeV were used in the fits.

Oscillations and fluctuations are evident in the data from [51] (Clement), [55] (Foster), and [54] (Larson). An assumption is made that these are artifacts, and that the net effect over a large enough range is that they wash out. The fluctuations in [51] (Clement) are quite large for energies below 2 MeV. Although they do not exceed the statistical errors for most of the data in that range, this portion of the data from [51] was omitted from the fits, as is suggested in [51]. The data from [54] (Larson) and [55] (Foster) seem to suffer similarly below 5 MeV, so this subset was also excluded. The 12 points from [51] above 18 MeV and the 9 points from [54] above 45 MeV have uncertainties approaching $\delta\sigma_{\text{crit}}$, and so were omit-

TABLE IV: The *np* total cross section data considered for the fits. N is the number of points in a publication. Values in the average χ^2 and average uncertainty (fraction of the measured value, standard deviation) columns are calculated from only the data below 15 MeV, except as noted. None of the data above 50 MeV were included in the fits. Only the data up to 3 MeV were used for the main results. The parameters used to calculate the average χ^2 are the shape-independent values from this work.

Ref.	First Author	N	Average unc. (perc.)	Average χ^2_ν	Min. energy (MeV)	Max. energy (MeV)
[12]	Koester	2	0.21	2.66	0.00197	0.143
[36]	Kirilyuk	2	0.14	0.407	0.002	0.145
[37]	Fujita	1	0.13	0.117	0.023645	0.023645
[38]	[a]Frisch	4	2.8	2.36	0.035	0.49
[39]	Allen	5	2.6	0.263	0.06	0.55
[40]	Bailey	15	3.8	0.971	0.35	6
[31]	[b]Engelke	2	0.25	2.7	0.4926	3.186
[41]	[b]Poenitz	3	0.3	2.35	0.509	2.003
[42]	[a]Cierjacks	1066	2	0.42	0.70145	31.99
[43]	Lampi	6	2.2	0.624	0.798	4.97
[44]	[a]Clements	17	0.46	4.59	0.841	19.957
[45]	[b]Fields	2	0.39	0.692	1.005	2.53
[46]	[a]Phillips	57	0.72	1.91	1.053	18.556
[47]	Koester	2	1.6	0.963	1.3	2.1
[48]	[b]Storrs	1	0.54	0.0321	1.312	1.312
[49]	Schwartz	1652	1.5	0.851	1.447	14.97
[50]	Davis	27	0.94	1.45	1.5	27.515
[51]	[c]Clement	166	0.98	1.12	2	17.976
[52]	[d]Nereson	38	10	0.0715	2.95	13.1
[53]	[b]Hafner	1	0.38	0.143	4.748	4.748
[54]	[e]Larson	342	1.6	0.96	5.0004	44.643
[55]	[f]Foster	111	2.1	1.17	5.012	14.689
[56]	[a]Bratenahl	6	1.8	4	7.17	14.02
[57]	Cook	8	1.7	0.977	14.1	18
[58]	[g]Bowen	63	4.8	2.97	15.8	111.5
[59]	[g]Peterson	5	2.3	5.69	17.8	29
[60]	[g]Groce	3	0.51	33.1	19.565	27.95
[61]	[g]West	5	3	0.873	19.58	30.46
[62]	[g]Brady	8	0.78	43.1	24.63	59.35
[63]	[g]Taylor	5	3.4	0.0302	38	153
[64]	[g]Lisowski	113	1.3	23.7	39	793
[65]	[g]Hillman	3	5.4	4.55	47.5	88

[a]Data not included in fits.
[b]Energy as adjusted by [66].
[c]The data below 2 MeV and above 18 MeV are excluded.
[d]Data included despite the large, 10% average uncertainty; the uncertainties appear to be overstated.
[e]The data below 5 MeV and above 45 MeV are excluded.
[f]The data below 5 MeV are excluded.
[g]Columns' values calculated with data up to 50 MeV.

ted. The data from [38] (Frisch), [44] (Clements), [46] (Phillips), and [56] (Bratenahl) are substantially deviant from the other data, as indicated by their large average χ^2, so they were excluded. Because of the apparent, systematic shift in the data from [42] (Cierjacks), compared to the other data, these data were excluded, despite their good, average χ^2 (which merely reflects that the stated uncertainties are large enough to include this shift). There are a few publications' data which were retained, despite seeming to be substantially deviant from other data, because they have only a few points (3 or less). For such small statistics, the average χ^2 per datum is not a reliable determination of their deviance. The data from publications which are all above 15 MeV were not excluded, despite the large, average χ^2 for some. A poor fit is expected for these because of contributions from higher waves. These data do not affect the main results, which involve only the data up to 3 MeV.

The results presented here depend on the particular choices made in the data selection process. Several alternative selections were made, where the more deviant data were not cut out. This resulted in parameter variations not entirely in agreement with the final values from this work. If the published uncertainties of the selected data are not too far off from being standard deviations (as may not be true for the excluded data), and if there are no systematic errors which approach or exceed the given uncertainties, then the measurements will be appropriately weighted and any likely selection bias affecting the resulting fit parameters will be reflected in the fit errors.

B. The S wave

The S wave partial cross section approaches a constant in the limit of zero energy, while the partial cross sections for the P, D, and all waves higher than S approach zero in this limit, i.e., $f_L \sim k^{2L}$ as $k \to 0$, where f_L is the amplitude for the wave with orbital angular momentum L. The contributions from higher angular momentum waves increase with energy, resulting in a decrease in the apparent effective range r_{s0} and an increase in χ^2_ν, if they are ignored. In order to maintain full model-independence, it is necessary to ignore the higher waves, but it is important to justify that ignoring them is valid for a usable range of low energy. Clearly, by ignoring higher waves, at any energy, systematic errors are introduced, but these will be seen to be much smaller than the statistical errors. As will be demonstrated in Sec. IV C, the need for any wave higher than S is not apparent from the data in the limit of zero energy (i.e., below 3 MeV with this data set).

Table V shows the partial cross sections, using the dominant phase shifts from Table V of [1] at 1, 5, 10, and 25 MeV, calculated from

$$\sigma(^{2S+1}L_J) = \pi(2J+1)k^{-2}\sin^2\delta(^{2S+1}L_J), \qquad (4.1)$$

which includes an integration over 4π solid angle and the statistical factor. S, L, and J are the spin, orbital, and total angular momentum of the *np* system. Mixing is ignored in (4.1). Taking into account D/S mixing (i.e., mixing of the $L = J-1$ and $L = J+1$ states for $J = 1$), represented by the $J = 1$ mixing angle ε_1, yields

$$\sigma(^3S_1) = \pi k^{-2}\Big(\tfrac{1}{2}\big|e^{2i\delta_1}\cos 2\varepsilon_1 - 1 - \tfrac{1}{\sqrt{2}}ie^{i(\delta_1+\delta_2)}\sin 2\varepsilon_1\big|^2 + \tfrac{1}{4}\big|e^{2i\delta_1}\cos 2\varepsilon_1 - 1 + \sqrt{2}\,ie^{i(\delta_1+\delta_2)}\sin 2\varepsilon_1\big|^2\Big) \qquad (4.2)$$

$$\sigma(^3D_1) = \pi k^{-2}\Big(\tfrac{1}{4}\big|e^{2i\delta_2}\cos 2\varepsilon_1 - 1 - \sqrt{2}ie^{i(\delta_1+\delta_2)}\sin 2\varepsilon_1\big|^2 + \tfrac{1}{2}\big|e^{2i\delta_2}\cos 2\varepsilon_1 - 1 + \tfrac{1}{\sqrt{2}}ie^{i(\delta_1+\delta_2)}\sin 2\varepsilon_1\big|^2\Big), \qquad (4.3)$$

where $\delta_1 = \delta(^3S_1)$ and $\delta_2 = \delta(^3D_1)$. These follow from Eqs. (16), (17), and (18) of [1]. Table V also shows the

TABLE V: The partial cross sections $\sigma(^{2S+1}L_J)$ calculated with (4.1) from the largest np phase shifts $\delta(^{2S+1}L_J)$ from Table V of [1] for 1, 5, 10, and 25 MeV. The $^3S_1$ and $^3D_1$ waves are treated both with $\varepsilon_1 = 0$, and with ε_1 from Table V of [1] with (4.2) and (4.3). The ratios $\sigma(^{2S+1}L_J)/\sigma$ with the total cross section use σ from this work. The ratios $\delta\sigma/\sigma$ are the relative (statistical) cross section errors, from this work.

Wave $^{2S+1}L_J$		$\delta(^{2S+1}L_J)$ (degrees)	$\sigma(^{2S+1}L_J)$ (b)	$\sigma(^{2S+1}L_J)/\sigma$
	For $T_L = 1$ MeV	$\sigma = 4.24855$ b	$\delta\sigma/\sigma = 0.00045$	
$^1S_0$		62.068	2.03536	0.47907
$^1P_1$		−0.187	0.00003	0.00000
$^3D_2$		0.006	0.00000	0.00000
$^3S_1$	$\varepsilon_1 = 0$	147.747	2.22778	0.52436
$^3S_1$	$\varepsilon_1 = 0.105$	147.747	2.22779	0.52437
$^3D_1$	$\varepsilon_1 = 0$	−0.005	0.00000	0.00000
$^3D_1$	$\varepsilon_1 = 0.105$	−0.005	0.00002	0.00001
	For $T_L = 5$ MeV	$\sigma = 1.62670$ b	$\delta\sigma/\sigma = 0.00048$	
$^1S_0$		63.63	0.41862	0.25734
$^1P_1$		−1.487	0.00035	0.00021
$^3D_2$		0.222	0.00004	0.00002
$^3S_1$	$\varepsilon_1 = 0$	118.178	1.21564	0.74730
$^3S_1$	$\varepsilon_1 = 0.672$	118.178	1.21552	0.74723
$^3D_1$	$\varepsilon_1 = 0$	−0.183	0.00002	0.00001
$^3D_1$	$\varepsilon_1 = 0.672$	−0.183	0.00023	0.00014
	For $T_L = 10$ MeV	$\sigma = 0.93502$ b	$\delta\sigma/\sigma = 0.00056$	
$^1S_0$		59.96	0.19540	0.20898
$^1P_1$		−3.039	0.00073	0.00078
$^3D_2$		0.846	0.00028	0.00030
$^3S_1$	$\varepsilon_1 = 0$	102.611	0.74496	0.79673
$^3S_1$	$\varepsilon_1 = 1.159$	102.611	0.74467	0.79642
$^3D_1$	$\varepsilon_1 = 0$	−0.677	0.00011	0.00012
$^3D_1$	$\varepsilon_1 = 1.159$	−0.677	0.00043	0.00046
	For $T_L = 25$ MeV	$\sigma = 0.36826$ b	$\delta\sigma/\sigma = 0.00080$	
$^1S_0$		50.90	0.06281	0.17057
$^1P_1$		−6.311	0.00126	0.00342
$^3D_2$		3.708	0.00218	0.00592
$^3S_1$	$\varepsilon_1 = 0$	80.63	0.30461	0.82714
$^3S_1$	$\varepsilon_1 = 1.793$	80.63	0.30432	0.82636
$^3D_1$	$\varepsilon_1 = 0$	−2.799	0.00075	0.00203
$^3D_1$	$\varepsilon_1 = 1.793$	−2.799	0.00105	0.00285

$^3S_1$ and $^3D_1$ partial cross sections from (4.2) and (4.3). Taking $\varepsilon_1 = 0$ in (4.2) and (4.3) yields (4.1) for both.

For perfect agreement between the cross sections from [1] and this work, the numbers in the last column of each section of Table V should add up to unity (counting the $^3S_1$ and $^3D_1$ only for one of the two values of ε_1). There is a small disagreement between the total cross section from this work and from [1], which is likely due to the use of the Dilg cross section there, which causes the low energy cross sections to be increased (see the Appendix).

C. The shape-independent fits

Table VI shows the results of fits of σ_0, a_c, and r_{s0} to the data set. The data were selected for each fit by cutting on the neutron (lab) kinetic energy at $T_{\max} = 50$, 40, 30, 20, 15, 10, 5, 4, 3, 2, 1 and 0.5 MeV. The generally too-good χ^2_ν reflect that most of the experimental uncertainties are overestimated. To correct this, the uncertainties from different publications would require different scaling factors to correct them. This is not done, since such a scaling would be biased by the results here, and would guarantee a good fit even with a poor set of parameters. It is preferred to regard the experimental uncertainties from their respective publications as preeminent, and thereby retain their utility in deciding whether or not to retain a given set of data, or whether or not the data are well-represented by the parameters for a given range of energy. So, the requirement for a "good" fit, that $\chi^2_\nu = 1 \pm \sqrt{2/\nu}$, must be interpreted somewhat loosely. The lowest energy fits, for data below 1.0 MeV, have very few degrees of freedom, and are especially susceptible to errors in this small subset of the data.

Only r_{s0} varies significantly amongst the fits below 15 MeV. The decline of r_{s0} and the increase in χ^2_ν with $T_{\max}$ above 5 MeV may reasonably be interpreted as being due to higher waves. Between 1 and 4 MeV, the variations in fit values of r_{s0} are not quite significant. The barely significant increase in r_{s0} between 4 MeV and 5 MeV could possibly be due to small errors in the data (contributions from higher waves should have the opposite effect). The 3 MeV fit is in the middle of the range over which r_{s0} is nearly constant (and where there is a good quantity of data), and is well below the region for which there is unmistakable evidence of higher waves. Furthermore, the 3 MeV fit has nearly the lowest χ^2_ν, while also having nearly the smallest errors for the fit parameters. Therefore, the best fit in Table VI is taken as the 3 MeV fit. Variations in the parameters from the 2 to 4 MeV fits are roughly the size expected from statistical fluctuations, and are not in the direction expected for them to be due to ignoring higher waves. Therefore, any systematic errors introduced by ignoring the higher waves are small compared to the statistical errors. Significant shape dependence as a function of energy (i.e., $\rho_{dk} \neq \rho_{d0}$) from 0 to 3 MeV is not evident, also because the variations are of the size expected for statistical fluctuations.

While these conclusions have merit by themselves, they are closely supported by Table V. The increase with energy in the higher waves in Table V shows good correspondence with the falloff in r_{s0} in Table VI. The first partial cross section (higher than S) comparable to the cross section uncertainty is the $^1P_1$ wave at 5 MeV. No wave higher than S in Table V at 1 MeV registers any contribution greater than 2% (1/45 for the $^3D_1$ wave) of the error in the cross section. The phase shifts for 3 MeV are not given in [1], but a conservative estimate, assuming the amplitudes scale like k^{2L} between 1 and 5 MeV, and taking the geometric average of the scaled 1 and 5 MeV partial cross sections for $^1P_1$ and $^3D_1$, puts the sum of those waves' contributions at 0.41 of the statistical error (standard deviation) in the 3 MeV cross section. At 2 MeV, that contribution has dropped to 0.10 of the statistical error. The net systematic contribution from ignoring the higher waves should therefore be much less than half the size of the statistical errors. The *rise* in r_{s0} from 0.5 to 5 MeV (ignoring higher waves should *reduce* r_{s0}) is indicative of systematic errors in this range of data. The large, systematic error on r_{s0} obtained in the

TABLE VI: 3-parameter (shape-independent) fits. The fit parameters are σ_0, a_c, r_{s0}, except for the last fit. The shape-independent singlet apparent effective range is $r_{s0} = \rho_{s0} - (\delta r_s)_{\Delta r_t}$, where $(\delta r_s)_{\Delta r_t}$ is the unknown systematic shift in r_{s0} from taking $\Delta r_t = 0$. The value of $T_{\max}$ shown is the highest energy in a data set. The errors on σ_0, a_c, r_{s0} are from the fitter, except for the last fit; the others are propagated from the fit errors using Table I. The fit chosen as the best fit is in boldface.

$T_{\max}$(MeV)	a_t (fm)	a_s (fm)	ρ_{tm} (fm)	r_{s0} (fm)	σ_0 (b)	a_c (fm)	χ^2_ν	ν
49.900	5.3851(12)	−23.6422(33)	1.7133(16)	2.5458(94)	20.2932(60)	−3.74343(95)	1.0734	2456
39.765	5.3913(12)	−23.6596(33)	1.7212(16)	2.6019(95)	20.3253(61)	−3.74277(95)	0.9995	2434
29.734	5.3959(12)	−23.6723(33)	1.7271(16)	2.6440(95)	20.3489(61)	−3.74228(95)	0.9653	2391
20.000	5.4053(12)	−23.6984(34)	1.7391(16)	2.7347(97)	20.3973(61)	−3.74130(96)	0.9079	2312
15.000	5.4082(12)	−23.7065(34)	1.7427(16)	2.7646(98)	20.4122(61)	−3.74100(96)	0.8847	2243
10.000	5.4113(12)	−23.7154(34)	1.7468(16)	2.802(10)	20.4287(61)	−3.74067(96)	0.8433	1945
5.000	5.4128(13)	−23.7193(37)	1.7486(17)	2.817(14)	20.4361(68)	−3.74053(98)	0.7991	1259
4.000	5.4118(14)	−23.7167(39)	1.7474(18)	2.786(15)	20.4313(72)	−3.74059(98)	0.7849	1078
3.000	**5.4114(15)**	**−23.7153(43)**	**1.7468(19)**	**2.754(18)**	**20.4287(78)**	**−3.7406(10)**	**0.7543**	**818**
2.000	5.4113(19)	−23.7151(54)	1.7467(24)	2.739(30)	20.4283(99)	−3.7406(10)	0.6705	390
1.000	5.4111(21)	−23.7143(61)	1.7464(27)	2.667(52)	20.427(11)	−3.7405(10)	1.2041	19
0.493	5.4105(21)	−23.7127(62)	1.7458(27)	2.574(61)	20.424(11)	−3.7405(10)	0.7025	13
Fit a_t, a_s, r_{s0}. Fit errors for a_t and a_s, and propagated errors for σ_0, a_c, and ρ_{tm}, are underestimated.								
3.000	5.41137(65)	−23.7153(20)	1.74682(83)	2.754(18)	20.4287(31)	−3.7406(14)	0.7543	818

TABLE VII: 4-parameter (shape-dependent) fits. The fit parameters are $\sigma_0, a_c, \rho_{t0}, \rho_{s0}$, except for the last fit. There is no systematic shift in ρ_{s0} from Δr_t. The fit errors for ρ_{t0} and ρ_{s0} are underestimated. This table is otherwise similar to Table VI.

$T_{\max}$(MeV)	a_t (fm)	a_s (fm)	ρ_{t0} (fm)	ρ_{s0} (fm)	σ_0 (b)	a_c (fm)	χ^2_ν	ν
49.900	5.4062(16)	−23.7000(46)	1.5777(37)	2.3357(94)	20.4005(84)	−3.7407(10)	0.8907	2455
39.765	5.4062(16)	−23.7002(46)	1.5836(37)	2.3508(95)	20.4010(84)	−3.7408(10)	0.8683	2433
29.734	5.4063(16)	−23.7004(46)	1.5865(38)	2.3584(96)	20.4013(84)	−3.7408(10)	0.8663	2390
20.000	5.4074(16)	−23.7037(46)	1.6154(38)	2.4391(98)	20.4074(84)	−3.7407(10)	0.8718	2311
15.000	5.4085(16)	−23.7069(46)	1.6360(38)	2.4993(99)	20.4132(84)	−3.7407(10)	0.8637	2242
10.000	5.4098(16)	−23.7105(46)	1.6542(39)	2.556(10)	20.4198(84)	−3.7406(10)	0.8309	1944
5.000	5.4113(17)	−23.7149(47)	1.6638(53)	2.599(14)	20.4281(87)	−3.7405(10)	0.7861	1258
4.000	5.4111(17)	−23.7142(48)	1.6792(63)	2.623(15)	20.4268(88)	−3.7405(10)	0.7770	1077
3.000	5.4110(18)	−23.7141(50)	1.7042(78)	2.661(18)	20.4266(92)	−3.7405(10)	0.7517	817
2.000	5.4109(20)	−23.7138(57)	1.671(19)	2.630(30)	20.426(10)	−3.7405(10)	0.6628	389
1.000	5.4107(21)	−23.7132(62)	1.57(12)	2.593(52)	20.425(11)	−3.7405(10)	1.2452	18
0.493	5.4107(22)	−23.7131(63)	1.85(16)	2.609(61)	20.425(11)	−3.7405(10)	0.7525	12
Fit ρ_{t0}, ρ_{s0} with fixed a_t, a_s from best fit of Table VI. This is taken as the best shape-dependent fit.								
3.000	5.4114(15)	−23.7153(43)	1.7051(78)	2.665(18)	20.4287(65)	−3.7406(31)	0.7511	815

next section supports this, and, in light of that systematic error, the significance of ignoring the higher waves is further (and drastically) reduced.

The shape-independent ERT parameters, the values of σ_0 and a_c, and the singlet binding energy (pole position) are determined to be

$$\begin{aligned} a_t &= 5.4114 \pm 0.0015 \text{ fm} \\ a_s &= -23.7153 \pm 0.0043 \text{ fm} \\ r_t &= \rho_t(0, -\epsilon_t) = 1.7468 \pm 0.0019 \text{ fm} \\ r_s &= r_{s0} = 2.754 \pm 0.018_{\text{stat}} \pm 0.056_{\text{syst}} \text{ fm} \\ \sigma_0 &= 20.4287 \pm 0.0078 \text{ b} \\ a_c &= -3.7406 \pm 0.0010 \text{ fm} \\ \epsilon_s &= 66.25 \pm 0.13 \text{ keV}. \end{aligned} \tag{4.4}$$

The errors are standard deviations, although no corrections have been made to account for the low value of χ^2_ν, so the errors might be oversized by roughly 10%. All the errors are statistical. The systematic error shown for r_s is explained in Sec. IV D. The error shown for ϵ_s is calculated using the larger, systematic error on r_s. None of the other parameters have significant systematic errors.

Note that the fit value of a_c is practically fixed to that of [34], because of its small uncertainty. The fit value of σ_0 is mostly determined by the 1.97 keV measurement from [12] and the 2 keV measurement from [36]. The σ_0 data [11, 31] have a fairly small effect on the fits.

A fit using a_t, a_s, and r_{s0}, instead of σ_0, a_c, and r_{s0}, is shown in Table VI to illustrate the correlation between a_t and a_s and its effect on the fit errors, as mentioned earlier. The values obtained for the parameters are the same, except that the errors for a_t, a_s, and ρ_{tm} are smaller by about a factor 2 (i.e., the errors for substantially correlated variables are underestimated by the fitter). The fit error on r_{s0} is the same in either case.

D. The shape-dependent fits

Fits were made in which r_t was fit, rather than being taken as ρ_{tm} from (3.5) with $\Delta r_t = 0$. When fit like this, r_t is the triplet (shape-dependent) apparent effective range, a determination of $\rho_{t0} \equiv \rho_t(0,0) = \lim_{T\to 0} \rho_t(0,T)$, and r_s is the singlet (shape-dependent) apparent effective range, a determination of $\rho_{s0} \equiv \rho_s(0,0) = \lim_{T\to 0} \rho_s(0,T)$, but without a systematic contribution from taking $\Delta r_t = 0$. These fits are shown in Table VII. These are called "shape-dependent" because they are done without the shape-independent approximation $\rho_{tk} = \rho_{tm}$. If the data were sufficiently precise (they are not), these fits would presumably show an energy dependence from neglecting the shape parameters in the effective range expansion (see Sec. V), in addition to the effects of higher waves (this is also true of r_{s0} in

the shape-independent fits). These fit values of ρ_{t0} and ρ_{s0} appear to be significantly different from the values of ρ_{tm} and r_{s0} of Table VI. The values of a_t and a_s differ insignificantly between Tables VI and VII (below 20 MeV). A fit varying only r_s and r_t, with a_t and a_s fixed to the best-fit values from Table VI, is shown at the bottom of Table VII, for the data up to 3 MeV, and this is taken as the best shape-dependent fit. This last fit omits the σ_0 and a_c data, since these data have no effect on this fit.

The apparent difference in Tables VI and VII between the values of ρ_{tm} and ρ_{t0}, and between r_{s0} and ρ_{s0}, is deceiving at this point, because the fit values of ρ_{t0} and ρ_{s0} are correlated, which means that their fit errors are underestimated. Figure 5 shows the effects on the ERT cross section of shifting r_t and r_s up, separately and in tandem, by amounts which anticipate the results below. (There is no particular reason for showing r_t and r_s shifted up, rather than down, which would have produced a similar, but inverted, set of curves.) The shift in cross section from about 2 MeV to 10 MeV is almost negligible if both r_s and r_t are shifted by those amounts. Therefore, cross sections in that range do not tightly constrain r_t and r_s if they are varied simultaneously. The shift in cross section increases above 10 MeV, but there the higher waves are significant and cannot be ignored. The shift in cross section is larger below 2 MeV, but there are not enough, precise data below 2 MeV to constrain r_t and r_s more than they already are by the data above 2 MeV. Thus, a substantial correlation exists between r_t and r_s. This correlation is *obscured* when r_s is fit with r_t fixed to ρ_{tm} (constrained by a_t). When r_t is fixed, the value of r_s is much more sensitive to the data above 2 MeV, as shown by the lower curve in Fig. 5. If the actual value of Δr_t is sufficiently close to zero, then fixing r_t to ρ_{tm} with a_t through (3.5), and varying r_s (as r_{s0}), will provide the best fit values for the ERT parameters (least affected by errors in the cross section data), but there remains an unknown contribution to r_{s0} from either a true, nonzero value of Δr_t (shape dependence), or, from errors in the data giving rise to a false, nonzero value of Δr_t (looks like shape dependence). In either case, the existence of this unknown contribution to r_{s0} is not apparent, so long as r_t and r_s are not varied simultaneously (and independently of a_t and a_s).

To obtain statistically meaningful errors for the fit values of ρ_{t0} and ρ_{s0}, one more type of fit is employed. The parameters a_t, a_s, ρ_{t0}, and ρ_{s0} are fixed at their values from the bottom of Table VII, and a new variable $\Delta\rho_t$, representing a perturbation in ρ_{t0}, is introduced as the sole fit parameter. The correlation between ρ_{s0} and ρ_{t0} is given by (3.10). The change $\Delta\rho_s$ in ρ_{s0} needed to (substantially) cancel the effect on χ^2_ν from the change $\Delta\rho_t$ in ρ_{t0} is given by $\langle \partial r_s/\partial\Delta r_t\rangle\,\Delta\rho_t$. Throughout the fit, ρ_{t0} and ρ_{s0} are varied according to

$$\rho'_{t0} = \rho_{t0} + \Delta\rho_t \qquad \rho'_{s0} = \rho_{s0} + \Delta\rho_t \left\langle \frac{\partial r_s}{\partial \Delta r_t} \right\rangle . \quad (4.5)$$

With this prescription, $\Delta\rho_t$ fits to a value of *zero*, but

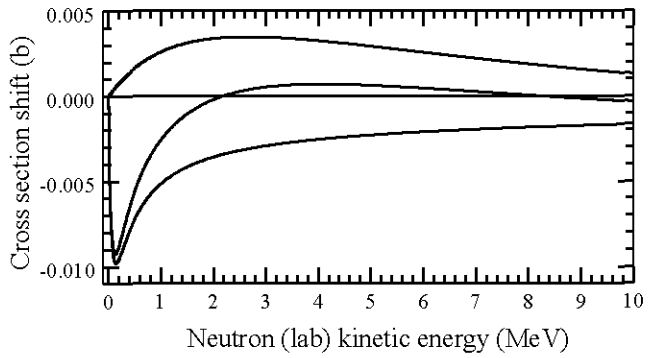

FIG. 5: The effects on the ERT cross section of shifting r_t up by 0.023 fm and r_s up by 0.056 fm, separately and in tandem.
Line at zero: ERT cross section, using the shape-independent parameters from this work.
Lower curve: only r_s is shifted.
Middle curve: r_s and r_t shifted in tandem.
Upper curve: only r_t is shifted.

its fit-error is not zero, and is correctly determined as a standard deviation if the errors in the data follow a Gaussian distribution and if $\chi^2_\nu = 1 \pm \sqrt{2/\nu}$. The mean value of $\partial r_s/\partial\Delta r_t$ is 2.3729, using the data of the best shape-dependent fit, at the bottom of Table VII. The fit has $\chi^2_\nu = 0.7502$, with $\nu = 816$. The fit-values from Table VII and the fit-errors from this $\Delta\rho_t$ fit, propagated through (4.5) for ρ'_{t0} and ρ'_{s0}, are

$$\begin{aligned} \rho_{t0} &\equiv \rho_t(0,0) = 1.705 \pm 0.023 \text{ fm} \\ \rho_{s0} &\equiv \rho_s(0,0) = 2.665 \pm 0.056 \text{ fm} \\ \Delta r_t &\equiv \rho_{t0} - \rho_{tm} = -0.042 \pm 0.024 \text{ fm}. \end{aligned} \quad (4.6)$$

With these uncertainties, which are considerably larger than those from Table VII, the differences between ρ_{tm} and ρ_{t0} and between r_{s0} and ρ_{s0} are not quite significant, being less than two standard deviations apart. The statistical error on ρ_{s0} is taken as the systematic error on r_s due to ignoring Δr_t.

V. DISCUSSION

The zero-energy shape dependence considered here (which is independent of energy) must be distinguished from the shape dependence which is more generally spoken of (which is dependent on energy). The (old) effective range expansion [17, 26, 67, 68] is

$$k\cot\delta_d = -a_d^{-1} + \tfrac{1}{2}\rho_{d0}k^2 - P_d\rho_{d0}^3k^4 + \ldots \quad (5.1)$$

The CFS [69] form is [26, 28, 67, 68]

$$k\cot\delta_d \cong -a_d^{-1} + \tfrac{1}{2}\rho_{d0}k^2 - p_dk^4/(1+q_dk^2). \quad (5.2)$$

The *Bethe equation* is

$$k\cot\delta_d = -a_d^{-1} + \tfrac{1}{2}\rho_{dk}k^2, \quad (5.3)$$

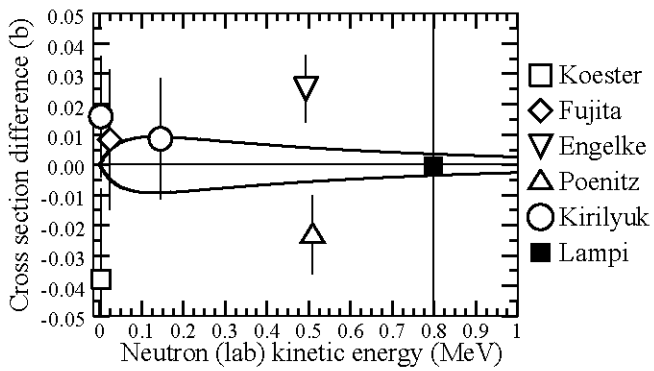

FIG. 6: Differences between the measured np total cross sections for the data below 1 MeV used in the fits, and the ERT calculation (measured - calculated).
Reference line at zero: Parameters from (4.4).
Lower curve: $r_t = \rho_{tm} + 0.023$ fm and $r_s = r_{s0} + 0.056$ fm.
Upper curve: $r_t = \rho_{tm} - 0.023$ fm and $r_s = r_{s0} - 0.056$ fm.
Data: [12] (Koester), [37] (Fujita), [31] (Engelke), [41] (Poenitz), [36] (Kirilyuk), and [43] (Lampi). The data which are off-scale are not shown (cf. Table IV).

which is exact, with $\rho_{dk} \equiv \rho_d(0,T)$. Then

$$\rho_{dk} \cong \rho_{d0} - 2p_d k^2/(1+q_d k^2) \tag{5.4}$$

$$\rho_{dk} \cong \rho_{dm} + \Delta r_d - 2p_d k^2/(1+q_d k^2), \tag{5.5}$$

using (2.8). The large, uncertain value of Δr_t determined here suggests that determinations of the spin-triplet shape-dependent coefficients p_t and q_t may suffer from considerable systematic errors, especially because Δr_t (as determined here) almost certainly represents errors in the data.

Remark on effective range expansions: The series (5.1) is not a theoretically justified form, and suffers from convergence problems, which the CFS form avoids. Whether a series such as (5.1) converges *well enough* depends on the range of energy and the precision of the available data; their coefficients are *inherently* dependent on the range of energy of the data, and have no physical significance. Historically, expansions in k^2 originated when high energies were not available and convergence was not an issue. Their continued, widespread use may have to do with the misconception that the k^2 term in the Bethe equation is the first-order term in a k^2 expansion, *which it is not*; the k^2 term has an *exact* origin in the Bethe equation [17]. *The effective range should never be expanded in a k^2 series.*

Figure 6 emphasizes how poorly determined are ρ_{t0}, ρ_{s0}, and therefore Δr_t, by the data available. Whether the reference line or one of the curves fits the data better can hardly be decided. The maximum separation between the upper and lower curves occurs at 131 keV; a simultaneous determination of ρ_{t0} and ρ_{s0} is most sensitive to a measurement at this energy. The sensitivity falls to half-maximum at 23 and 620 keV. Figure 6 shows that the useful data between 23 keV and 620 keV are very sparse. More precise data in this region would greatly improve the situation: a single cross section with a precision of 0.4 mb near 131 keV would reduce the errors on ρ_{t0} and Δr_t to about 0.001 fm. As it stands, Δr_t is more a measure of errors in the data than a measure of zero-energy shape dependence.

Potential models predict various differences between $\rho_t(0,0)$ and $\rho_t(0,-\epsilon_t)$, and there is much to be gained from comparing such predictions with the experimental difference, as obtained by the model-independent analysis described here. For the present, Δr_t is insufficiently well-determined to be of any use in such a comparison. The mutual relation, or correlation, between experimentally determined values of $\rho_s(0,0)$ and $\rho_t(0,0)$ has a mutually degrading effect on their determinations, and therefore also on $\Delta r_t \equiv \rho_t(0,0) - \rho_t(0,-\epsilon_t)$. The improved low-energy cross section measurements required to overcome this degrading effect, in order that this analysis may bear its full fruit, are not exceedingly difficult to make, nor costly, and may have lacked only a motive to make them. It is hoped that this motive is now provided, and that this old well is not quite so dry as may have been supposed.

Acknowledgments

I am grateful to R. Chrien for his many helpful comments on the draft. This work was supported by the United States Department of Energy, under Contract No. DE-AC02-98CH10886.

APPENDIX: THE ZERO-ENERGY FREE PROTON CROSS SECTION AND THE DILG MEASUREMENT

Consider a neutron beam scattering on a proton target. The cross section σ as given by (2.2) with (2.1) is the free proton cross section, which is the elastic cross section which would be measured if the struck protons were not bound in molecules. The zero-energy free proton cross section σ_0 is given by (3.1). For neutron energies well above the vibrational level-spacing, the inelastic molecular contributions from vibrational excitations can be handled by introducing a molecular-vibration correction factor [70–72]. The total cross section becomes

$$\sigma_{\rm tot} = \sigma_0(1 + A/T_L) + (\sigma - \sigma_0) + \sigma_{M1}. \tag{A.1}$$

The $(\sigma - \sigma_0)$ term represents the change in cross section with neutron (lab) kinetic energy T_L, from (2.2). σ_{M1} is the $M1$ radiative neutron capture cross section. The parameter A is a function of the molecular makeup, and it depends on the temperature. The parameter A may be nearly constant over some ranges of energy, but generally depends on the energy in a manner which requires a substantial theoretical effort to predict. In measurements of the cross section, A is determined by a fit to a

subset of the data which is well-described by a constant A. While the fit value of A for a given target composition at a given temperature shows reasonable agreement with theory (when calculations exist), the agreement is not generally excellent, and it is the fit value of A which is employed in the reduction of the data to determine σ_0. The top two entries in Table II were obtained with this technique.

If the data set is restricted to energies sufficiently above molecular binding energies, the proton can be treated as free, and σ_0 obtained by extrapolating (or fitting) with (2.4). If the energies are low enough such that the uncertainties in the effective ranges have little effect on the result, the extrapolation does not contribute significantly to the error. The last entry in Table II and the result from this work both fall into this category.

The Dilg measurement of σ_0 [10] used an energy at which the molecular correction term $\sigma_0 A/T_L$ in (A.1) should be small but not quite negligible, and should nearly cancel with the $(\sigma - \sigma_0)$ term. The result in [10] follows from measurements on water and three hydrocarbons at a single energy, 132 eV. There was, therefore, no way of determining A, as was done in [30] and [11]. Instead, A was estimated for each target from values taken from the literature, which described scattering on water and benzene at energies from about 1 to 15 eV. The resulting corrections were extrapolations to 132 eV.

The Dilg σ_0 is unique in that it is the only measurement which required molecular corrections to be made but did not obtain them as part of the experiment. If the molecular corrections for the different targets were underestimated, the resulting value for σ_0 would be too large (and the error too small), which seems to be the case. All other experiments, whether requiring molecular corrections or not, have produced results in good agreement with each other, and this includes fits to the low energy measurements above 2 keV. It is inconceivable that the Dilg result is correct while all others are not, especially in light of its unique handling of the molecular corrections.

[1] V. G. J. Stoks, R. A. M. Klomp, M. C. M. Rentmeester, and J. J. de Swart, Phys. Rev. C **48**, 792 (1993).

[2] V. Stoks and J. J. de Swart, Phys. Rev. C **52**, 1698 (1995).

[3] R. Machleidt and I. Šlaus, J. Phys. G **27**, R69 (2001).

[4] R. B. Wiringa, V. G. J. Stoks, and R. Schiavilla, Phys. Rev. C **51**, 38 (1995).

[5] R. Machleidt, F. Sammarruca, and Y. Song, Phys. Rev. C **53**, R1483 (1996).

[6] S. Nakamura, T. Sato, V. Gudkov, and K. Kubodera, Phys. Rev. C **63**, 34617 (2001).

[7] R. Schiavilla, V. G. J. Stoks, W. Glöckle, H. Kamada, A. Nogga, J. Carlson, R. Machleidt, V. R. Pandharipande, R. B. Wiringa, A. Kievsky, et al., Phys. Rev. C **58**, 1263 (1998).

[8] G. Q. Li and R. Machleidt, Phys. Rev. C **58**, 3153 (1998).

[9] G. A. Miller, M. K. Nefkens, and I. Šlaus, Phys. Rep. **194**, 1 (1990).

[10] W. Dilg, Phys. Rev. C **11**, 103 (1975).

[11] T. L. Houk, Phys. Rev. C **3**, 1886 (1971).

[12] L. Koester, W. Waschkowski, and J. Meier, Z. f. Physik **A 337**, 341 (1990).

[13] O. Dumbrajs, R. Koch, H. Pilkuhn, G. C. Oades, H. Behrens, J. J. de Swart, and P. Kroll, Nucl. Phys. **B 216**, 277 (1983).

[14] L. Koester and W. Z. Nistler, Z. f. Physik **A 272**, 189 (1975).

[15] S. Klarsfeld, J. Martorell, and D. W. L. Sprung, J. Phys. G **10**, 165 (1984).

[16] R. Machleidt, Phys. Rev. C **63**, 24001 (2001).

[17] H. A. Bethe, Phys. Rev. **76**, 38 (1949).

[18] J. M. Blatt and V. F. Weisskopf, *Theoretical Nuclear Physics* (Wiley, NY; Chapman & Hall, London, 1952).

[19] R. Wilson, *The Nucleon-Nucleon Interaction, Experimental and Phenomenological Aspects* (Interscience, New York, 1963).

[20] Equation (2.2) is not usually written as a single equation, except in [19]. Usually, one finds $\sigma_d = 4\pi k^{-2}\sin^2\delta_d$, with $k\cot\delta_d$ given by (5.3), both of which are exact.

[21] The phrase "mixed effective range" [10, 11, 68] is nothing more than a convenient name for $\rho_d(0, -\epsilon_d)$, appropriate because in this case (2.3) is a mixture of neutron-proton and deuteron wavefunctions.

[22] L. P. Kok, Phys. Rev. Lett. **45**, 427 (1980).

[23] Occasionally in the literature there is something like $a_c = (3a_t + a_s)/4\mu$, e.g. [1], where μ is the $\mathbf{H}_2$ molecular mass correction, $\mu \approx \frac{1}{2}$. This is not correct. a_c is *defined* by (3.2), or $a_c \equiv 2(\frac{3}{4}a_t + \frac{1}{4}a_s)$, where the factor 2 arises because there are two indistinguishable protons. The molecular mass correction correctly occurs in the relation between the coherent cross section and a_c. See [18, 19, 73].

[24] Particle Data Group, Phys. Lett. B **592**, 1 (2004).

[25] E. G. Kessler et al., Phys. Lett. A **255**, 221 (1999).

[26] H. P. Noyes, Phys. Rev. **130**, 2025 (1963).

[27] P. R. Bevington, *Data Reduction and Error Analysis for the Physical Sciences* (McGraw-Hill, New York, 1969), 1st ed., pg. 238.

[28] J. R. Bergervoet, P. C. van Campen, W. A. van der Sanden, and J. J. de Swart, Phys. Rev. C **38**, 15 (1988).

[29] E. Lomon and R. Wilson, Phys. Rev. C **9**, 1329 (1974).

[30] E. Melkonian, Phys. Rev. **76**, 1744 (1949).

[31] C. E. Engelke, R. E. Benenson, E. Melkonian, and J. M. Lebowitz, Phys. Rev. **129**, 324 (1963), data retrieved from the CINDA database, file EXFOR 11118.002 and 11118.003 dated 14 August 1980.

[32] L. Koester and W. Nistler, Phys. Rev. Lett. **27**, 956 (1971).

[33] J. Calleraine, D. J. Larson, S. J. Lipson, and R. Wilson, Phys. Rev. C **12**, 1423 (1975).

[34] V. F. Sears, Z. f. Physik **A 321**, 443 (1985).

[35] Nuclear Data Centers Network, **CINDA, Index to the Literature and Computer Files on Microscopic Neutron Data**, (International Atomic En-

ergy Agency, Vienna, Austria, 2004). Information extracted from the CINDA database, version 2004, http://www.nndc.bnl.gov/index.jsp, as of 1 September 2004. Target: H-1, H-BNZ, H-CMP, H-CXX, H-MTH, H-PFN, H-PHL, H-PLE, H-WTR; Reaction: N,TOT; Energy from 0 to 1000 MeV; EXFOR format. At the time the data were obtained from the NNDC, the data from [74] did not appear. Since those data are for energies above 9 MeV, and since the main results from the current work are determined from the data up to 3 MeV, the analysis was not repeated with those data.

[36] A. L. Kirilyuk, A. V. Grebnev, P. N. Vorona, and N. L. Gnidak, **C87KIEV2**, 298 (1987), data retrieved from the CINDA database, file EXFOR 40980.004 dated 29 August 1989.

[37] Y. Fujita, K. Kobayashi, T. Oosaki, and R. C. Block, Nucl. Phys. **A 258**, 1 (1976).

[38] D. H. Frisch, Phys. Rev. **70**, 589 (1946), data retrieved from the CINDA database, file EXFOR 11141.002 dated 14 August 1980.

[39] W. D. Allen and A. T. G. Ferguson, Proc. Phys. Soc. (London) **A 68**, 1077 (1955), data retrieved from the CINDA database, file EXFOR 21364.002 dated 4 November 1980 and 21364.003 dated 22 February 1980.

[40] C. D. Bailey et al., Phys. Rev. **70**, 583 (1946), data retrieved from the CINDA database, file EXFOR 11140.002 dated 14 August 1980.

[41] W. P. Poenitz and J. F. Whalen, Nucl. Phys. **A 383**, 224 (1982), data retrieved from the CINDA database, file EXFOR 12715.002 dated 27 January 1982.

[42] S. Cierjacks, P. Forti, G. J. Kirouac, D. Kopsch, L. Kropp, and J. Nebe, Phys. Rev. Lett. **23**, 866 (1969), data retrieved from the CINDA database, file EXFOR 20015.002 dated 1 September 1983.

[43] E. E. Lampi, G. D. Freier, , and J. H. Williams, Phys. Rev. **80**, 853 (1950), data retrieved from the CINDA database, file EXFOR 12644.003 dated 13 March 1979.

[44] P. J. Clements and A. Langsford, Phys. Lett. **30B**, 25 (1969), data retrieved from the CINDA database, file EXFOR 21497.002 dated 22 July 1981.

[45] R. E. Fields, R. L. Becker, and R. K. Adair, Phys. Rev. **94**, 389 (1954), data retrieved from the CINDA database, file EXFOR 11073.002 dated 6 January 1982.

[46] T. W. Phillips, B. L. Berman, and J. D. Seagrave, Phys. Rev. C **22**, 384 (1980), data retrieved from the CINDA database, file EXFOR 10945.002 dated 22 December 1982.

[47] L. Koester, W. Waschkowski, J. Meier, G. Rau, M., and Salehi, Z. f. Physik **A 330**, 387 (1988), data retrieved from the CINDA database, file EXFOR 22105.002 dated 3 February 1989.

[48] C. L. Storrs and D. H. Frisch, Phys. Rev. **95**, 1252 (1954).

[49] R. B. Schwartz, R. A. Schrack, and H. T. Heaton, Phys. Lett. **30B**, 36 (1969), data retrieved from the CINDA database, file EXFOR 10005.003 dated 17 June 1999.

[50] J. C. Davis and H. H. Barschall, Phys. Rev. C **3**, 1798 (1971), data retrieved from the CINDA database, file EXFOR 10099.003 dated 13 October 1999.

[51] J. M. Clement, P. Stoler, C. A. Goulding, and R. W. Fairchild, Nucl. Phys. **A 183**, 51 (1972), data retrieved from the CINDA database, file EXFOR 10173.003 dated 14 December 2000.

[52] N. Nereson and S. Darden, Phys. Rev. **89**, 775 (1953), data retrieved from the CINDA database, file EXFOR 11060.002 dated 6 January 1982.

[53] E. M. Hafner, W. F. Hornyak, C. E. Falk, G. Snow, and T. Coor, Phys. Rev. **89**, 204 (1952).

[54] D. C. Larson, J. A. Harvey, and N. W. Hill, ORNL **5787**, 174 (1980), data retrieved from the CINDA database, file EXFOR 12882.002 dated 4 September 1996.

[55] D. G. Foster, Jr., and D. W. Glasgow, Phys. Rev. C **3**, 576 (1971), data retrieved from the CINDA database, file EXFOR 10047.002 dated 7 September 1999.

[56] A. Bratenahl, J. M. Peterson, and J. P. Stoering, Phys. Rev. **110**, 927 (1958), data retrieved from the CINDA database, file EXFOR 11155.002 dated 14 August 1980.

[57] C. F. Cook and T. W. Bonner, Phys. Rev. **94**, 651 (1954), data retrieved from the CINDA database, file EXFOR 11074.002 dated 6 January 1982.

[58] P. H. Bowen, J. P. Scanlon, G. H. Stafford, J. J. Thresher, and P. E. Hodgson, Nucl. Phys. **22**, 640 (1961), data retrieved from the CINDA database, file EXFOR 21103.003 dated 11 April 1980.

[59] J. M. Peterson, A. Bratenahl, and J. P. Stoering, Phys. Rev. **120**, 521 (1960), data retrieved from the CINDA database, file EXFOR 11108.002 dated 14 August 1980.

[60] D. E. Groce and B. D. Sowerby, Nucl. Phys. **83**, 199 (1966), data retrieved from the CINDA database, file EXFOR 31278.002 dated 6 July 1984.

[61] M. L. West, C. M. Jones, and H. B. Willard, ORNL **3778**, 94 (1965), data retrieved from the CINDA database, file EXFOR 11031.002 dated 6 January 1982.

[62] F. P. Brady, W. J. Knox, J. A. Jungerman, M. R. McGie, and R. L. Walraven, Phys. Rev. Lett. **25**, 1628 (1970), data retrieved from the CINDA database, file EXFOR 10102.002 dated 2 February 2000.

[63] A. E. Taylor and E. Wood, Philos. Mag. **44**, 95 (1953), data retrieved from the CINDA database, file EXFOR 21378.002 dated 22 February 1980.

[64] P. W. Lisowski, R. E. Shamu, G. F. Auchampaugh, N. S. P. King, M. S. Moore, G. L. Morgan, and T. S. Singleton, Phys. Rev. Lett. **49**, 255 (1982), data retrieved from the CINDA database, file EXFOR 12761.002 dated 20 March 1985, and 12761.003 dated 20 February 1985.

[65] P. Hillman, R. H. Stahl, and N. F. Ramsey, Phys. Rev. **96**, 115 (1954), data retrieved from the CINDA database, file EXFOR 11081.002 and 11081.003 dated 6 January 1982.

[66] J. C. Davis and H. H. Barschall, Phys. Lett. **27B**, 636 (1968).

[67] H. P. Noyes and H. M. Lipinski, Phys. Rev. C **4**, 995 (1971).

[68] H. P. Noyes, Ann. Rev. Nucl. Sci. **22**, 465 (1972).

[69] M. Cini, S. Fubini, and A. Stanghellini, Phys. Rev. **114**, 1633 (1959).

[70] R. G. Sachs and E. Teller, Phys. Rev. **60**, 18 (1941).

[71] E. Melkonian, Phys. Rev. **76**, 1750 (1949).

[72] T. L. Houk and R. Wilson, Rev. Mod. Phys. **39**, 546 (1967).

[73] J. M. Blatt, Phys. Rev. **74**, 92 (1948).

[74] W. P. Abfalterer, F. B. Bateman, F. S. Dietrich, R. W. Finlay, R. C. Haight, and G. L. Morgan, Phys. Rev. C **63**, 44608 (2001), data retrieved from the CINDA database, file EXFOR 13753.032 dated 12 February 2004.